

Journal of Materials Chemistry A

Accepted Manuscript



This is an *Accepted Manuscript*, which has been through the Royal Society of Chemistry peer review process and has been accepted for publication.

Accepted Manuscripts are published online shortly after acceptance, before technical editing, formatting and proof reading. Using this free service, authors can make their results available to the community, in citable form, before we publish the edited article. We will replace this *Accepted Manuscript* with the edited and formatted *Advance Article* as soon as it is available.

You can find more information about *Accepted Manuscripts* in the [Information for Authors](#).

Please note that technical editing may introduce minor changes to the text and/or graphics, which may alter content. The journal's standard [Terms & Conditions](#) and the [Ethical guidelines](#) still apply. In no event shall the Royal Society of Chemistry be held responsible for any errors or omissions in this *Accepted Manuscript* or any consequences arising from the use of any information it contains.

In-situ synthesis of ternary BaTiO₃/MWNTs/PBO electromagnetic microwave absorption composites with excellent mechanical properties and thermostability

Cite this: DOI: 10.1039/x0xx00000x

Received 00th January 2012,
Accepted 00th January 2012

DOI: 10.1039/x0xx00000x

www.rsc.org/

Jia Wei^a, Shuo Zhang^b, Xiaoyun Liu^a, Jun Qian^{a*}, Jiasong Hua^a, Xinxin Li^a and Qixin Zhuang^{a*}

Abstract. Different from traditional microwave absorbing nanoparticles as fillers in non-mechanical coatings, the BaTiO₃/MWNTs/PBO ternary composites can be potentially used as structural microwave absorption device in broader prospects, especially in aerospace industry. BaTiO₃ particles with diameter of 5–15nm were immobilized onto surface of MWNTs via solvothermal synthesis. BaTiO₃/MWNTs/PBO ternary composites with varied compositions were then prepared via in-situ polymerization of p-phenylenebenzobisoxazole(PBO) with uniform dispersion of BaTiO₃/MWNTs nanocomposites in the polymer-poly p-phenylenebenzobisoxazole(PBO)-matrix, a conjugate polymer with splendid mechanical and thermal stability. The BaTiO₃/MWNTs/PBO composites possessed outstanding microwave absorbing performances in addition to desirable mechanical properties and thermal stability.

Introduction.

The inevitable and unprecedented electromagnetic radiation introduced by the rapid development of electronic technology has become one of the most serious pollutions. Therefore, researches on electronic microwave absorption materials have attracted intensive attentions on improvement of intensity loss of electromagnetic radiation. Additionally, the microwave absorption materials play a key role in electromagnetic shielding technical of aircraft in military fields¹⁻⁴.

It has been demonstrated that nanometer-scaled MWNTs is a remarkably high-performance functional microwave absorption material due to⁵⁻⁶ microscopic dimension effect, macroscopic quantum orbital effect, negative resistance and other characteristics of MWNT. The electronic microwave energy can effectively transfer or dissipate to electric, thermal or magnetic energy through MWNTs⁷⁻¹⁰. In order to further improve the absorption performance, MWNTs were modified with other absorbers such as metal particles (Fe, Ni, Ag etc.)¹¹⁻¹³, conductive polymers (polyaniline)¹⁴⁻¹⁶, nano-scaled ceramic (SiC, SiO₂, BaTiO₃,)¹⁷⁻²⁰ and ferrite (Fe₂O₃ and Fe₃O₄)²¹⁻²³ etc.²⁴⁻²⁶ Traditional studies were reported on coatings such as epoxy resin²⁷, polyurethane²⁸, and PVDF²⁹⁻³⁰, blending with absorbers without mechanical properties and low decomposition temperature under the 350. In the previous study of our group²¹, the γ -Fe₂O₃/MWNT/PBO was reported as a high efficiency microwave absorption composite with thermally stability over

400°C owing to poly (p-phenylenebenzobisoxazole) (PBO)³¹ possessing not only desirable thermal stability but also mechanical properties and environmental stability³²⁻³³. To the best of our knowledge, few studies were reported the microwave absorb composites with both outstanding mechanical property and thermal stability.

In this article, the surface of MWNTs was modified with nano-sized low-density BaTiO₃, possessing high dielectric constant and environmental stability, via efficient solvothermal method. Then the microwave-absorbing ternary BaTiO₃/MWNTs/PBO composite was fabricated via in-situ polymerization of PBO, and uniform dispersion of the BaTiO₃/MWNTs could be thus achieved. With an overall performance, the reflection loss reached the -45.5dB with MWNTs/BaTiO₃ (12%wt) at 9.7GHz and the widest absorbing bandwidth obtained is ranging from 7.5GHz-15.7GHz covering both higher and lower frequency superior to pure BaTiO₃/MWNTs nanoparticles. It was reported¹⁹ that the highest reflection loss (RL) of the BaTiO₃/MWNTs nanoparticle obtained then was -37.5 dB at a frequency of 10.4 GHz, and under -10 dB in the frequency range of 9.6–13.1 GHz range. The utmost tensile strength of the ternary BaTiO₃/MWNTs/PBO composites could be as high as 145.9MP, 122.1% higher than pure PBO film. In addition, the composites were thermally stable over 660 °C, potentially useful in extreme environment for long period, such as in the field of aircraft of complex condition.

This is so far the most effective microwave-absorbing composites with balanced mechanical and thermal properties as

well as environmental friendly properties, due to the special morphological and structures features of the BaTiO₃/MWNTs nanocomposites, and the synergistic effects of MWNTs and BaTiO₃.

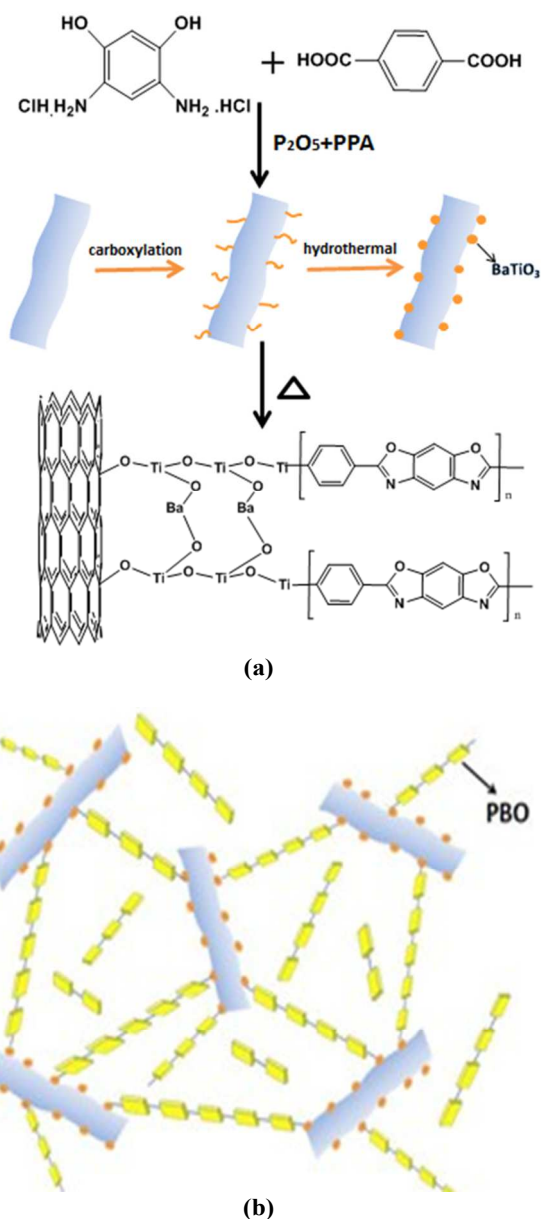
Experimental

4, 6-Diaminoresorcinol dihydrochloride (DAR.2HCl) was chemically synthesized according to the previous reports³⁴. Terephthalic acid (TPA) was purchased from Shanghai Reagents and ground to powder in a glove box prior to use. Methanesulfonic acid (MSA) was obtained from Sigma-Aldrich Chemical. Polyphosphoric acid (PPA), phosphorus pentoxide (P₂O₅), tetrabutyl titanate(Ti(OC₄H₉)₄), barium acetate(Ba(CH₃COO)₂) and other chemicals and solvent were from Lingfeng Shanghai Reagents Co. Ltd. (China). MWNTs were provided by Nachen Beijing Co. Ltd.(China).

Preparation of BaTiO₃/MWNTs nanocomposites via solvothermal synthesis. 0.6g MWCNTs were oxidized by HNO₃ at 120 °C for 24hours³⁵. The product was washed copiously with deionized water with high-speed centrifuge until the supernatant was neutral, and then collected with Buchner funnel followed by drying 60 °C. The oxidized MWNTs, 0.82g titanium hydroxide (obtained through hydrolyzing 2.4g Ti(OC₄H₉)₄ in ammonia) and 1.8g Ba(CH₃COO)₂ were added into mixed solution containing 30mL NH₂CH₂CH₂OH and 30mL NH₂CH₂CH₂NH₂, and pH was adjusted to 12 by addition of NaOH. The dispersion was transferred to a 100mL sealed Teflon lined hydrothermal synthesis autoclave reactor, and the reactor was kept at 200 °C in an oven for 12hours. The slurry was centrifuged subsequently and washed copiously with deionized water, 0.1M HCl and ethanol respectively until the supernatant was completely clear. The slurry was then dried at 60 °C for 24 hours to obtain the power.

Synthesis of BaTiO₃/MWNTs/PBO ternary composites via in-situ polymerization of DAR·2HCl and TPA.

BaTiO₃/MWNTs/PBO composites were prepared via polycondensation between DAR.2HCl and TPA in the presence of BaTiO₃/MWNTs. A typical procedure for preparation of BaTiO₃/MWNTs/PBO (with mass ratio of 95/5) composite was described as follows: 3g (14.1mmol) DAR·2HCl, 2.37g(14.1mmol) TPA, 30.9 g PPA (80.6wt% P₂O₅), 11.89 g P₂O₅, and BaTiO₃/MWNTs were added into a 250mL glass vessel equipped with a mechanical stirrer and nitrogen inlet/outlet. Subsequently, the mixture was mechanically stirred at 90 °C under nitrogen for 12 hours for complete removal of hydrochloride. The mixture was stirred at 110 °C under vacuum for additional 24hours, followed by being heated to 150 °C gradually at rate of 5-10 °C/hour, and kept at this temperature for another 12hours under continuous stirring. The crude product was poured into distilled water, and purified by Soxhlet extraction. The BaTiO₃/MWNTs/PBO composites in the water phase and were dried at 100 °C for 24h. PBO was also prepared in the absence of BaTiO₃/MWNTs for control purpose. This process was schematically shown in scheme 1.



Scheme 1. Synthetic strategy of BaTiO₃/MWNTs/PBO composites (a) and the sketch map of the ternary composite(b)

Characterizations and measurements

FTIR. The successful synthesis of BaTiO₃/MWNTs, PBO, and BaTiO₃/MWNTs/PBO composites were confirmed by Nicolet Magna-IR550 FTIR analyzer using KBr disk method,

X-ray diffraction (XRD). (from Rigaku D/max 2550V with Cu K_α radiation).

Morphology and microstructure. BaTiO₃/MWNTs and BaTiO₃/MWNTs/PBO were probed by transmission electron microscopy (TEM) (JEOL-2100F) and field emission scanning electron microscopy (FE-SEM) (Hitachi S-4800).

Thermo gravimetric analysis (TGA). Performed on a DuPont 1090B thermal gravimetric analyzer at heating rate of 10 °C·min⁻¹ under nitrogen stream (20mL min⁻¹).

Mechanical properties. BaTiO₃/MWNTs/PBO composites were measured by Instron HY-0230. Tensile tests were

performed on dog-bone-shape specimens at constant cross-head velocity of 5mm/min at ambient temperature.

Microwave measurements. The specimens were fabricated with 80 wt% the above composite and 20 wt% paraffin wax, because the paraffin wax is microwave-transparent and thus low in permittivity and permeability. The mixture was then pressed into hollow cylinders with outer diameter of 7 mm, inner diameter of 3 mm and thickness of 3 mm. The microwave parameters of the samples, complex permittivity and permeability, were measured by a vector network analyzer (Agilent 8505D) with testing frequency ranging from 2 to 18GHz. The reflection loss (RL) was calculated from the measured parameters according to the transmission line theory.

Results and discussion

XRD patterns of BaTiO₃, BaTiO₃/MWNTs nanocomposite and BaTiO₃/MWNTs/ PBO composites.

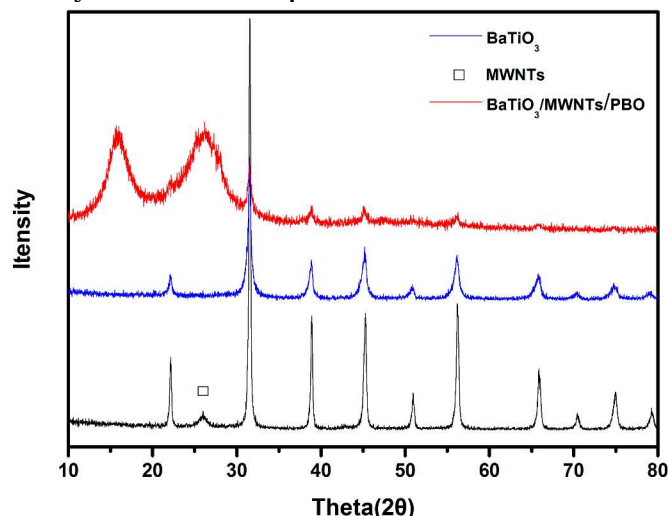


Figure 1. XRD spectra of BaTiO₃, BaTiO₃/MWNTs and BaTiO₃/MWNTs/PBO composites.

X-ray diffraction profiles of the BaTiO₃, BaTiO₃/MWNTs and BaTiO₃/MWNTs/PBO composites were presented in Fig. 1. Compared to pure BaTiO₃, the diffraction peaks of BaTiO₃/MWNTs nanocomposite at 26.3° confirmed the presence of MWNTs, well resolved from other sharp signals corresponding to XRD profiles of BaTiO₃ (JCDPS file No.31-0174). The BaTiO₃ was in its cubic crystal form in the BaTiO₃/MWNTs and free of impurities such as BaCO₃. As for BaTiO₃/MWNTs/PBO ternary composites, signals at 15.68° (200) and 25.44° (010) indicated the presence of partially order structure of PBO. It was known that the diffraction of pure PBO is in 26.46° (010), the slight position shift resulted from the rigid molecular motif into the composite. Although PBO polymer matrix was about 95% (wt) in mass, the characteristic peaks of BaTiO₃/MWNTs could still be identified, indicating its partial coverage by PBO. In addition, similar XRD profiles could be observed for BaTiO₃/MWNTs/PBO nanocomposites with other constitutions, well in accordance with the FTIR results.

FTIR patterns of BaTiO₃/MWNTs nanocomposite and BaTiO₃/MWNTs/ PBO composites.

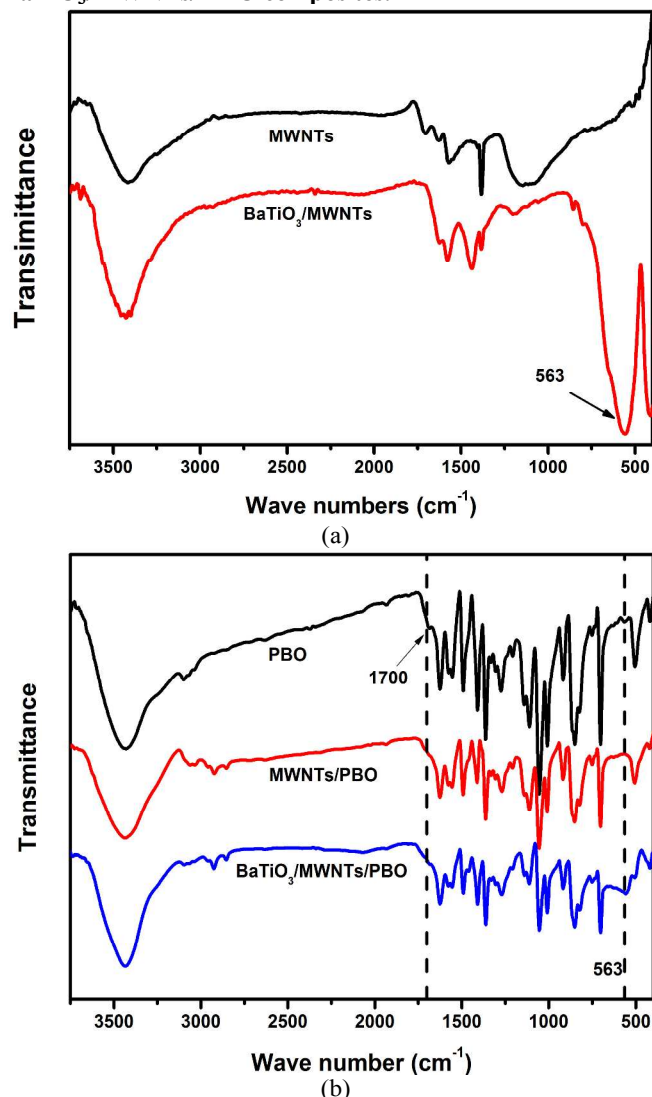


Figure 2. FTIR spectra of MWNT, BaTiO₃/MWNTs (a) nanocomposites; PBO, MWNTs/PBO, BaTiO₃/MWNTs/PBO (b) polymer composite

FTIR spectra of MWNT, BaTiO₃/MWNTs hybrid material, PBO, MWNTs/PBO, BaTiO₃/MWNTs/PBO were presented in Figure 2. Strong absorption at 563cm⁻¹ was observed in clearly observed in spectra of BaTiO₃/MWNTs compared to that of MWNTs, confirming the presence of BaTiO₃ as concluded from XRD. Similar characteristic absorption could be identified in the IR spectra of BaTiO₃/MWNTs/PBO at 566 cm⁻¹.

The structural integrity of PBO was confirmed by the presence of formation of characteristic absorption of C=N peaks at 1,624cm⁻¹ and that of C_{Ar}-N at 1,362 cm⁻¹ on the benzoxazole ring in PBO, MWNTs/PBO and BaTiO₃/MWNTs/PBO composite. Characteristic absorption of carbonyl group at 1700cm⁻¹, was observed in the spectra of PBO, yet in spectra of neither MWNTs/PBO nor BaTiO₃/MWNTs/PBO, indicative of successful synthesis of PBO in BaTiO₃/MWNTs/PBO via in-situ polymerization and chemical bonding between BaTiO₃ and PBO. The absence of chemical bonding in MWNTs/PBO could also be identified by the presence of absorption from the carbonyl group of PBO. An

illustration scheme was thus proposed to describe the preparation process of BaTiO₃/MWNTs/PBO.

Morphology of BaTiO₃/MWNTs nanocomposite and BaTiO₃/MWNTs/ PBO composite

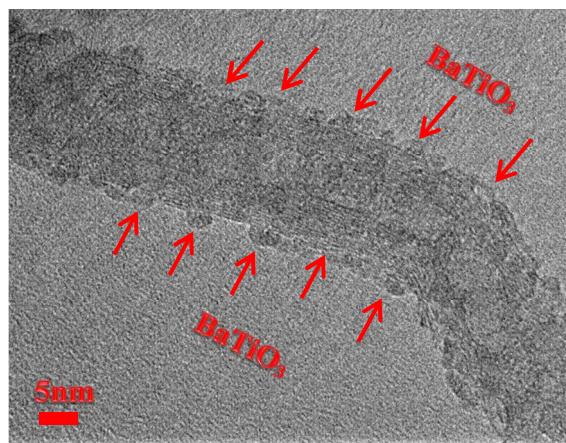
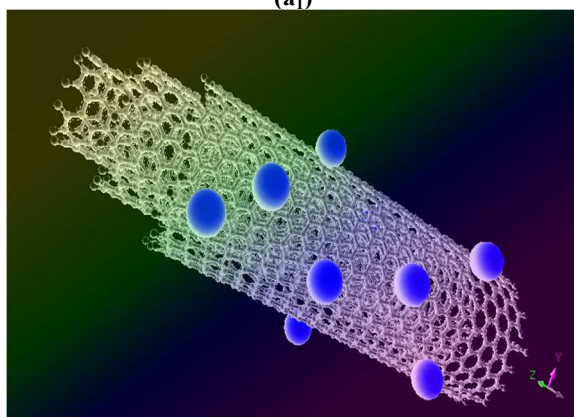
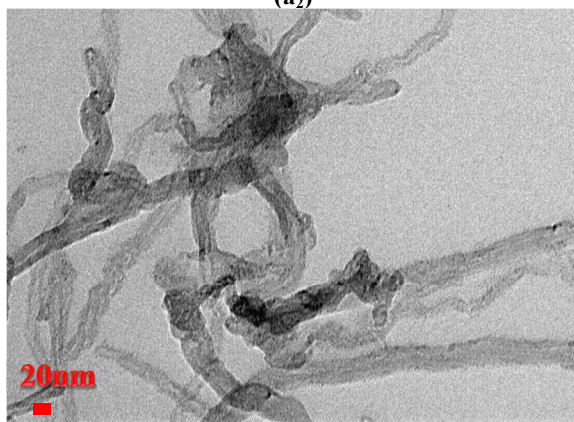
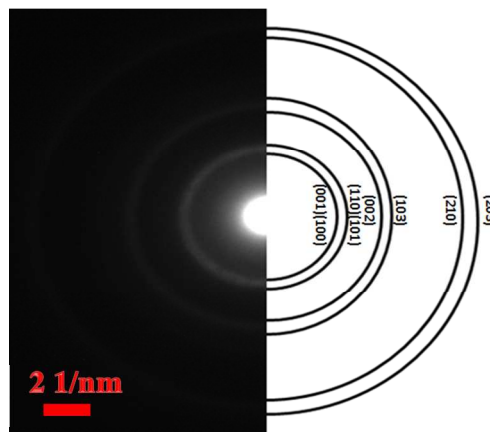
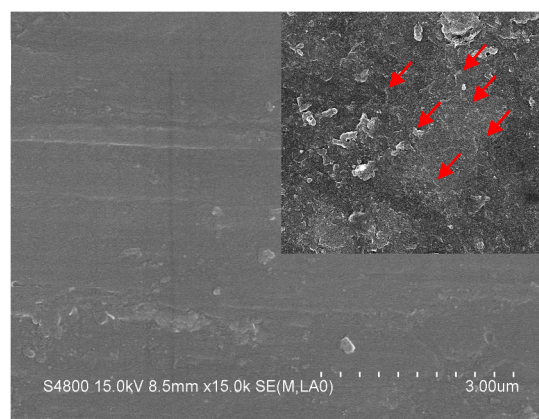
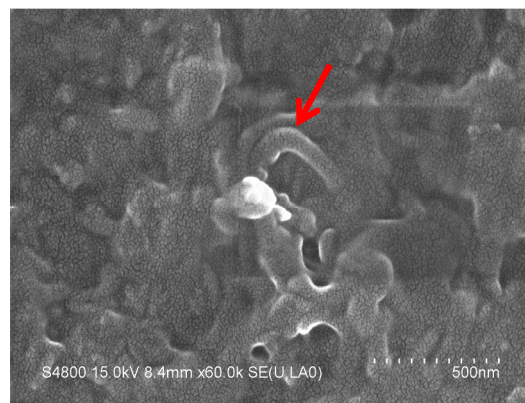
(a₁)(a₂)(b₁)(b₂)

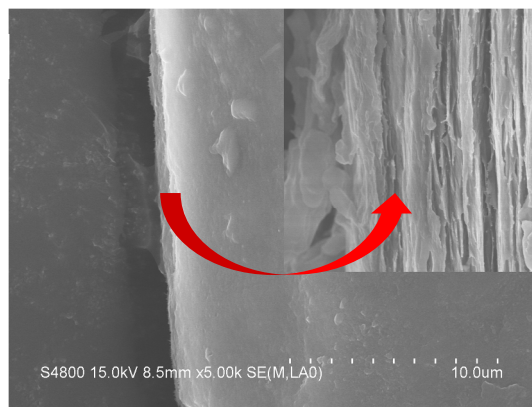
Figure 3. The TEM images of BaTiO₃/MWNTs (a₁) and the sketch image of BaTiO₃/MWNTs (a₂); The selected area electron area (b₁) and the SEAD diffraction (b₂);



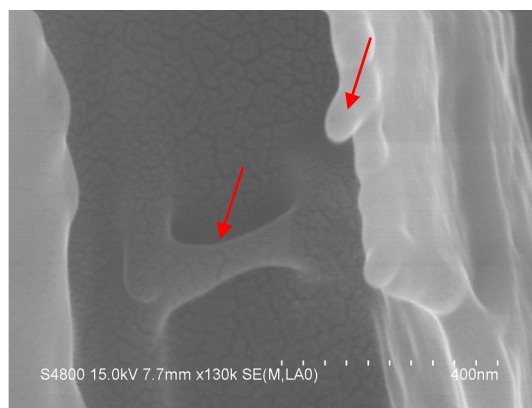
(c)



(d)



(e)



(f)

Figure 4. The SEM images of surface morphology of pure PBO and the BaTiO₃/MWNTs/PBO composites(c and d); The SEM images of the fracture surface of composite film(e and f).

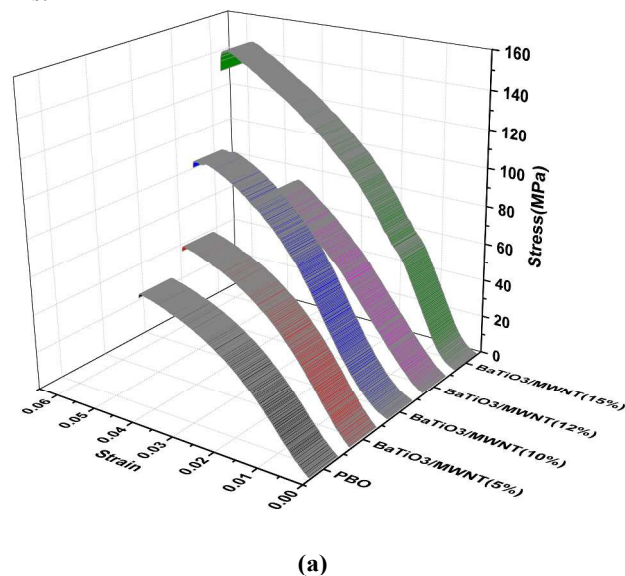
MWCNTs with diameter about 40nm were decorated by well-dispersed particles of BaTiO₃ with diameter about 5nm, as shown in bright-field TEM images (a₁) and the sketch image (a₂). Additionally, the selected-area electron diffraction (SAED) taken from an area containing a large amount of nanotubes (b₁) and it confirmed the identity of the nanoparticles and the characteristic spacing were indicative of the cubic perovskites structure of BaTiO₃(b₂) on the sidewalls of MWNTs, in good agreement of the XRD results.

The fibril morphological features with comparably higher brightness in SEM images could be interpreted as charging from poorly conductive BaTiO₃ arranging evenly on MWNTs, and were distributed randomly throughout the PBO matrix, as observed in figure 4 (c). Compared to neat PBO, uniform dispersion of BaTiO₃/MWNTs could be achieved in PBO matrix, and the borders of each phase could not be observed in SEM images of BaTiO₃/MWNTs/PBO, illustrating commendable compatibility of the three components in the ternary composite. In addition, SEM images of BaTiO₃/MWNTs/PBO at higher magnification presented in figure 4. (d) indicated that the PBO covering the surface of BaTiO₃/MWNTs network served as bridge to bind the nanocomposites firmly. In the figure 4. (e) and (f), the cross sections of the composites propagated layer by layer, and the adjacent layers were interconnected by BaTiO₃/MWNTs, reinforcing the tensile property of the films.

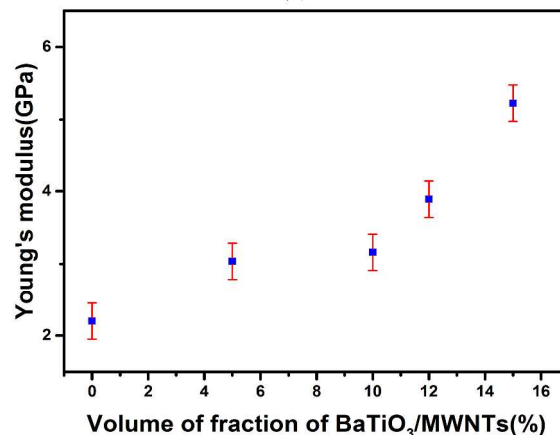
Additionally, on the edge of BaTiO₃/MWNTs/PBO composites, some MWNTs stretched out densely, and were tightly covered by PBO matrix, possibly resulting from the uniform distribution. It can be therefore concluded that, (1) MWNTs could be decorated by spherical BaTiO₃ with unambiguous edges via solvothermal treatment and high crystallinity as confirmed by XRD; (2) chemical bonding between BaTiO₃/MWNTs nanoparticles and PBO matrix contributed to the structural integrity of the composites, as supported by FTIR and TGA.

Graphics should be inserted where they are first mentioned (unless they are equations, which appear in the flow of the text). They can be single column or double column as appropriate.

Mechanical Properties of BaTiO₃/MWNTs/PBO Composite Films.



(a)



(b)

Figure 5. (a) Stress-strain curves for the BaTiO₃/MWNTs/PBO films with varied BaTiO₃/MWNTs-loading (wt%), (b) Plots of Young's modulus of the MWNT/PBO films with respect to the volume fractions of BaTiO₃/MWNTs



Figure 6. Tensile testing samples of the PBO and BaTiO₃/MWNTs/PBO films with specified BaTiO₃/MWNTs-loading (wt%).

The mechanical properties of BaTiO₃/MWNTs/PBO films were recorded in Figure 5. The stress-strain curves (a) of the films and the Young's modulus (b) of the neat PBO and BaTiO₃/MWNTs/PBO composites with different BaTiO₃/MWNTs loading were recorded, respectively. Neglecting the added mass of BaTiO₃/MWNTs, the presence of BaTiO₃/MWNTs led to an increase in stress compared to the neat PBO, and the stress at failure gradually improved by more than 100% to 145.9 MPa (BaTiO₃/MWNTs/PBO 15%wt), compared to 65.7 MPa of PBO. The areas under the stress-strain curves were integrated as the fracture work of composites, and were compared with respect to volume fractions of BaTiO₃/MWNTs. The improved fracture toughness was observed in the presence of BaTiO₃/MWNTs, and the highest with BaTiO₃/MWNTs/PBO (15%wt). The enhanced elongation upon addition of BaTiO₃/MWNTs attributed to chemical bonding between a BaTiO₃/MWNTs and PBO matrix. As of Young's modulus, the value increased from 2 GPa to over 5 GPa, and this could be interpreted as the bridging effect of BaTiO₃/MWNTs. It was reported²³ that the effective stress transfer was recognized in the polymer/CNT interface, and therefore the BaTiO₃/MWNTs could serve as a bridge to prevent the break down under stress during elongation. To conclude, the mechanical property of PBO could be reinforced by the effective interfacial interaction between the PBO and BaTiO₃/MWNTs, and homogeneous dispersion of the BaTiO₃/MWNTs in a PBO matrix, maximizing the area of the load transfer on the interface.

TGA patterns of BaTiO₃/MWNTs nanocomposite and BaTiO₃/MWNTs/PBO composites.

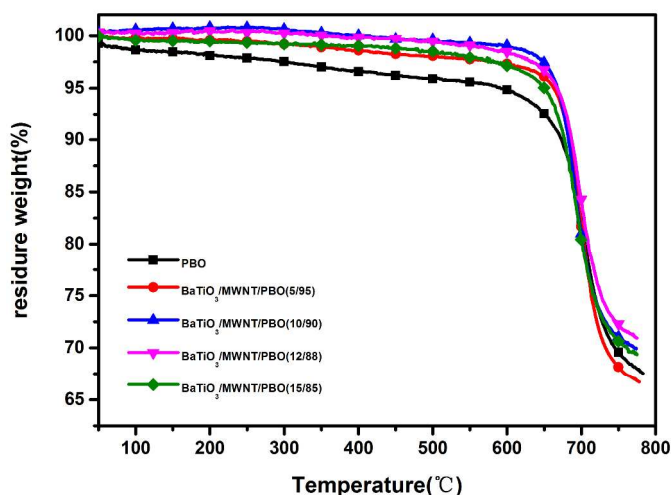


Figure 7. TGA curves of PBO and BaTiO₃/MWNTs/PBO composites

Table 1. Thermo stability of PBO and BaTiO₃/MWNTs/PBO composites

Sample ID	Temperature at which residual mass reached 95%	Residual mass at 650 °C (%)	Residual mass (%)
PBO	591	92	67
BaTiO ₃ /MWNTs/PBO (5%wt)	662	96	66
BaTiO ₃ /MWNTs/PBO (10%wt)	667	97	69
BaTiO ₃ /MWNTs/PBO (12%wt)	667	96	71
BaTiO ₃ /MWNTs/PBO (15%wt)	650	95	69

The thermal degradation behaviors of PBO and BaTiO₃/MWNTs/PBO ternary composites were studied via TGA, as recorded in fig 7. Under nitrogen atmosphere, apparent mass loss was hardly observed below 660 °C and the residual mass ratio of BaTiO₃/MWNTs/PBO ranged from 95% to 97% compared to only 92% for PBO, indicative of the remarkable thermal stability of BaTiO₃/MWNTs/PBO composites in extremely high temperatures. In addition, BaTiO₃/MWNTs/PBO composites started degradation (at 95 % mass loss) above 650 °C, well exceeding 591 °C for the neat PBO, as shown in table 1. This improvement could be possibly interpreted as the covalent chemical bonding.

Dielectric parameters of the PBO, MWNTs/PBO, and BaTiO₃/MWNTs/PBO composites

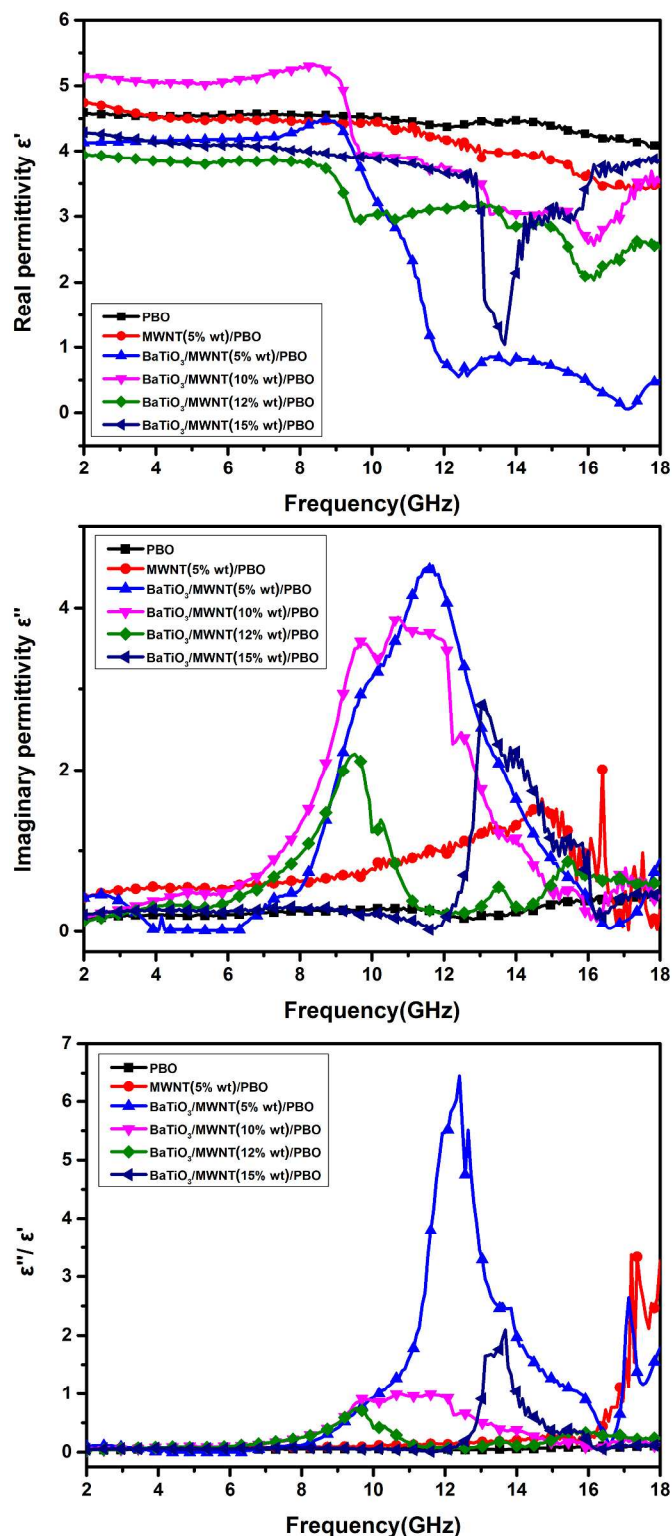


Figure 8. Dielectric parameters of PBO and the BaTiO₃/MWNTs/PBO composites with different ratio of BaTiO₃/MWNTs (a,b,c)

The frequency dependence of relative complex permittivity parameters, real part ϵ' , imaginary part ϵ'' and dielectric loss tangent ($\tan\delta_E = \epsilon''/\epsilon'$), of the PBO and the BaTiO₃/MWNTs/PBO ternary composites with different ratios of BaTiO₃/MWNTs were recorded respectively in figure 8. In a relative complex permittivity, ϵ' and ϵ'' represent the storage

and loss capability in response to microwave energy, and a rise in ϵ'' is attributed to microwave absorption. As shown in figure 8 (a), both the real part ϵ' and imaginary part ϵ'' of the complex permittivity for the neat PBO remained almost constant over the frequency range of interest, resulting in negligible dielectric loss tangent ($\tan\delta_E$). Upon addition of MWNTs, the dielectric parameters changed dramatically. Similar characteristics were shown in the figures of other samples except for the one with 15%wt BaTiO₃/MWNTs. For the rest samples, ϵ' dropped in a gradient manner with increasing loading of BaTiO₃/MWNTs, beginning from around 5 at 8GHz and extending to around 2 at 16 GHz, over the two microwave absorption regions. Additionally, the ϵ'' of these samples significantly increased from where the ϵ' started to decrease, and finally reached the peak around 10GHz, in a wide frequency range. The dielectric loss tangent curves exhibited similar behavior as the ϵ'' curve. Due to the absence of magnetic constituents, the real part and imaginary part of complex permeability were about 1.0 and 0.0, respectively. However, the single value of permittivity or permeability cannot describe the microwave absorbing properties directly, and therefore, the impedance matching and further calculation of reflection loss must be considered seriously.

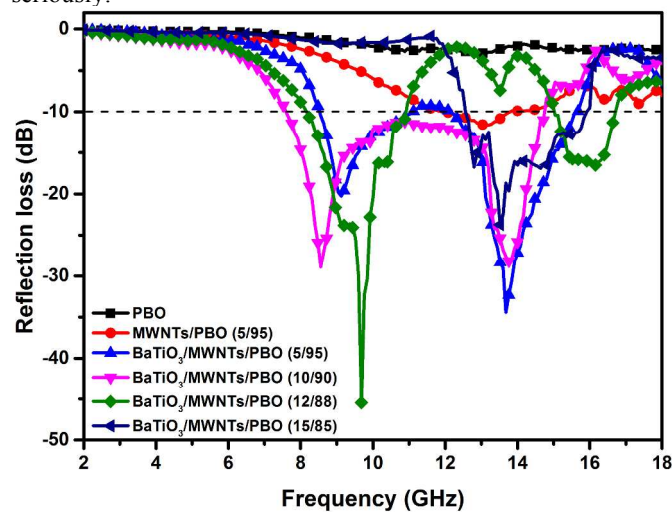
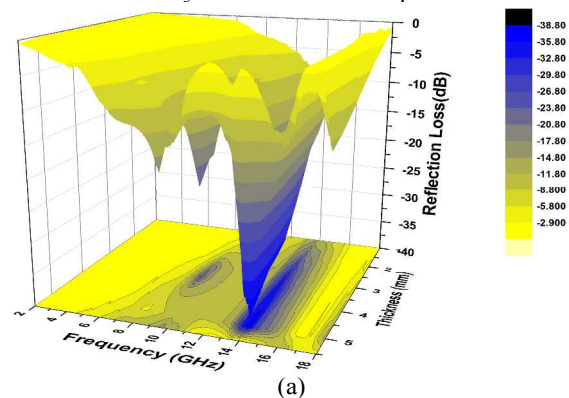


Figure 9. Microwave RL for the PBO, MWNTs/PBO, and BaTiO₃/MWNTs/PBO composites



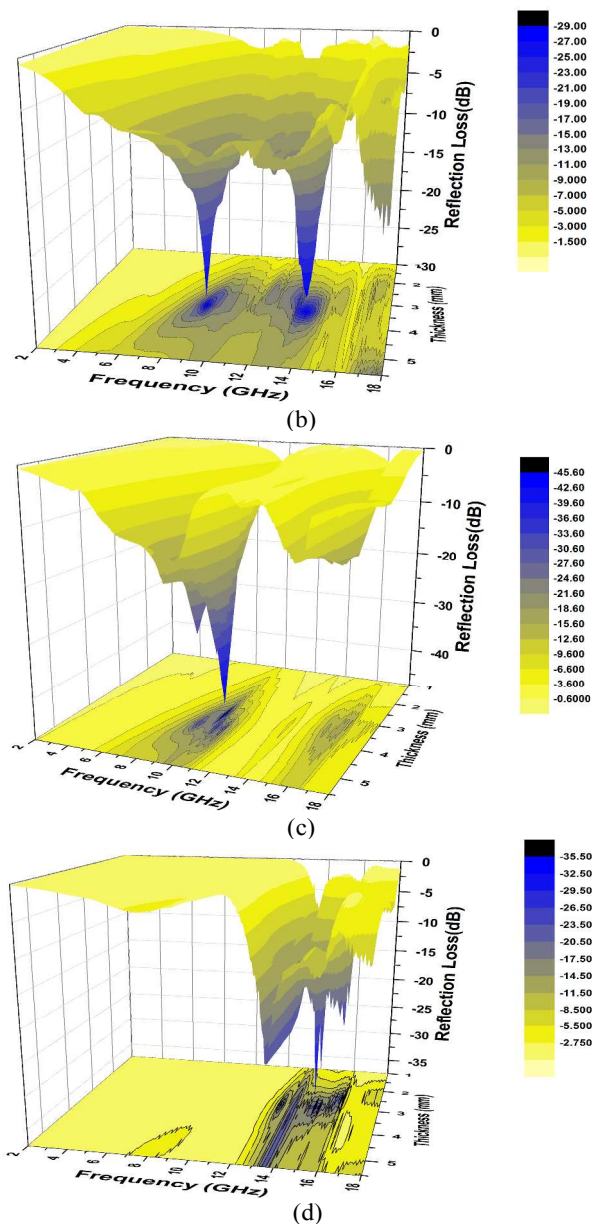


Figure 10 Three dimensional and contour plot of the RL versus 5wt%(a) 10wt%(b) 12wt%(c) 15wt%(d) BaTiO₃/MWNTs with different thickness

BaTiO₃/MWNTs According to the theory of electromagnetism absorption, the reflection loss (RL) of samples shown in fig can be calculated using the formulas below:

$$RL(dB) = 20 \log \left| \frac{Z_n - 1}{Z_n + 1} \right|$$

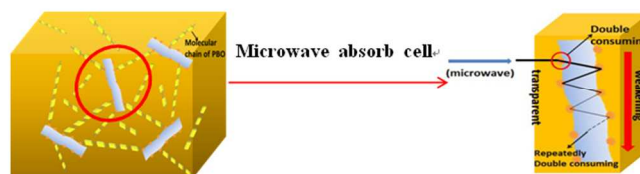
$$Z_{in} = \sqrt{\frac{\mu}{\epsilon}} \tanh \left[j \left(\frac{2\pi f t}{c} \right) \sqrt{\mu \epsilon} \right]$$

where c , f and t are the velocity of the electromagnetism wave, the frequency of the electromagnetism wave and the wall thickness of the absorber, respectively. The ϵ and μ are the

complex permittivity and complex permeability tested by network analyzer. The thickness of each sample was 3 mm. Fig. 10 shows the three dimensional plots and contour plots of reaction loss (RL) in different thickness.

As shown in figure 9, it could be identified that the neat PBO barely had any microwave absorption at RL values less than -5dB. The addition of 5%wt MWNTs could improve the value mildly to -10 dB at most. Nonetheless, in the presence of BaTiO₃/MWNTs, RL-frequency plot for BaTiO₃/MWNTs/PBO composites demonstrated the analogous dual-region curves except for the sample with 15%wt BaTiO₃/MWNTs. For the sample with 5wt% BaTiO₃/MWNTs/PBO, the RL-frequency curve had two peak values, -20dB at 9 GHz and -35dB at 13.7GHz respectively. With increasing BaTiO₃/MWNTs fraction, the optimal RL peak value at lower frequency gradually increase from -20dB to -45dB (12%wt), and that at higher frequency decrease from -35dB to -16dB (12%wt). However, for the composite with 15%wt of BaTiO₃/MWNTs, RL-frequency curve with random fluctuation was observed similar to that of MWNTs/PBO, possibly due to non-uniform dispersion of BaTiO₃/MWNTs. The effective microwave absorption bandwidth ranged widely from 7.5 GHz to 15 GHz particularly at moderate concentration of 10wt %. To conclude compared to MWNTs, the unique synergistic effect of BaTiO₃ nanoparticles and MWNTs could enhance the microwave absorbing behavior of PBO significantly in a wide frequency range with dual-region in optimal ratio. Low feed of BaTiO₃/MWNTs contributed to absorption in lower frequency range, and higher fraction of BaTiO₃/MWNTs contributed to the absorption in higher frequency range. Different from other microwave absorbing coatings, the thickness of the BaTiO₃/MWNTs/PBO composites polymers were not among the prioritized concerns, because this kind of materials could be processed as structural support instead of coatings.

Microwave absorbing mechanism of BaTiO₃/MWNTs/PBO composite



Scheme 2. Microwave absorbing mechanism for BaTiO₃/MWNTs/PBO composite

It was reported³⁶⁻³⁷ that microwave energy could be consumed by transformation into other kinds such as electric energy, magnetic or heat energy via different mechanisms in microwave absorbers. MWNTs³⁸⁻⁴⁰ with high length-to-radius ratio is a microwave absorber of intense research interests, primarily attributed to the pores, lattice distortions and dangling bonds, and therefore microwave can be repeatedly polarized to trigger dielectric loss. In addition, according to the energy band theory, when the size of conductive material was reduced to nanometer scale⁴¹, the original quasi-continuous energy spectrum will split into discrete energy levels, which happened to overlap with the range of microwaves, and this offered a novel gap for microwave absorption. When BaTiO₃/MWNTs/PBO become a homogeneous dielectric medium, it can produce multiple resonance absorption over a wide microwave band.

For the MWNTs decorated by BaTiO₃ nanoparticles, quantum size effect and the polarization effect of

MWNTs/BaTiO₃⁴²⁻⁴³ were enhanced markedly, and the incident microwaves could thus be scattered and consumed repeatedly, superior to direct dispersion of MWNTs and BaTiO₃ in the polymer separately. For the MWNT-based polymer composites, the geometry of particles and the dispersion had dramatic impact on microwave absorption. According to kinetic theory of percolation, percolation threshold was influenced by aspect ratio, surface modification and the dispersion of MWNTs in polymer matrix. In this system, as shown in scheme 2, the MWNTs/BaTiO₃ interacted with each other via tunneling effect, and the large aspect ratio introduced strong polarization effect, and resulted in formation of conductive channel. The BaTiO₃ nanoparticles, on the other hand, efficiently concerted with synergistic polarization instead of a not a simple superposition among each component, and nano effect of MWNTs, and therefore, the microwave transformed into dielectric and electric energy.

The fraction of MWNTs/BaTiO₃ had great influence on the impedance matching and the microwave absorption properties of the ternary composite. It was illustrated that with increasing loading of MWNTs/BaTiO₃, two adjacent nano-scaled tubes tended to bind to each other, forming a larger particle, more effective in absorption in low frequency range instead of high frequency. In a certain range, low dose of MWNTs/BaTiO₃ led to high-frequency microwave absorption, while higher dose of MWNTs/BaTiO₃ led to low-frequency microwave absorption, but beyond that range, the RL-frequency curves behaved abnormally due to possible conglomeration. The theory of impedance matching is too complicated to be interpreted, until now there is no explicit designing guidance⁴⁰⁻⁴¹. This study may offer additional perspectives on designing multi-element and multi-layer microwave absorption materials.

Conventionally, the microwave-absorbing materials were applied as coatings, such as epoxy resin. Compared to epoxy resin, the conjugated PBO matrix offers a smoother channel for charge transfer. Accordingly, the microwave could be efficiently transferred to absorbers via the PBO matrix. With the synergistic effect of MWNTs, BaTiO₃ and PBO, the composites were proved to be effective in absorbing microwaves in a wide range with low RL values, and have great potential in further application. The mechanism of underlying this microwave-absorbing composite will be studied intensively in the near future, and additional applications will be explored.

Conclusions

The MWNTs/BaTiO₃/PBO ternary microwave-absorbing composites with varied fractions of MWNTs/BaTiO₃ have been successfully synthesized by in-situ polymerization with chemical bonding between PBO and BaTiO₃. The MWNTs/BaTiO₃ nanocomposites were fabricated by solvothermal method. Compared to neat PBO and MWNTs/PBO (5 wt %), the ϵ' and ϵ'' of MWNTs/BaTiO₃/PBO changed dramatically when fabricated into ternary composites, possible attributed to the enhanced interfacial polarization of MWNTs/BaTiO₃. The maximum value of reflection loss (RL) was achieved at -45.5dB with 12%wt MWNTs/BaTiO₃ at 9.7GHz and the widest bandwidth was obtained ranging from 7.5GHz-15.7GHz. The utmost stress of composites reached 145.9MPa (122.1% improvement compared to PBO) and onset of thermal degradation could be beyond 660°C. To best of our knowledge, this is the first example demonstrating remarkable structural microwave absorbing material associated with the excellent mechanical and thermo stability properties. This strategy is effective in promoting the microwave absorption in

materials. Additional optimization, such as modification of MWNTs-based absorbers, compounding condition, etc., would give rise to improved mechanical, thermal and microwave absorption properties of the hybrid composites. The material demonstrated in this study is a promising candidate for aerospace application as structural scaffold to satisfy the demands in extreme frequency ranges or over a wide bandwidth.

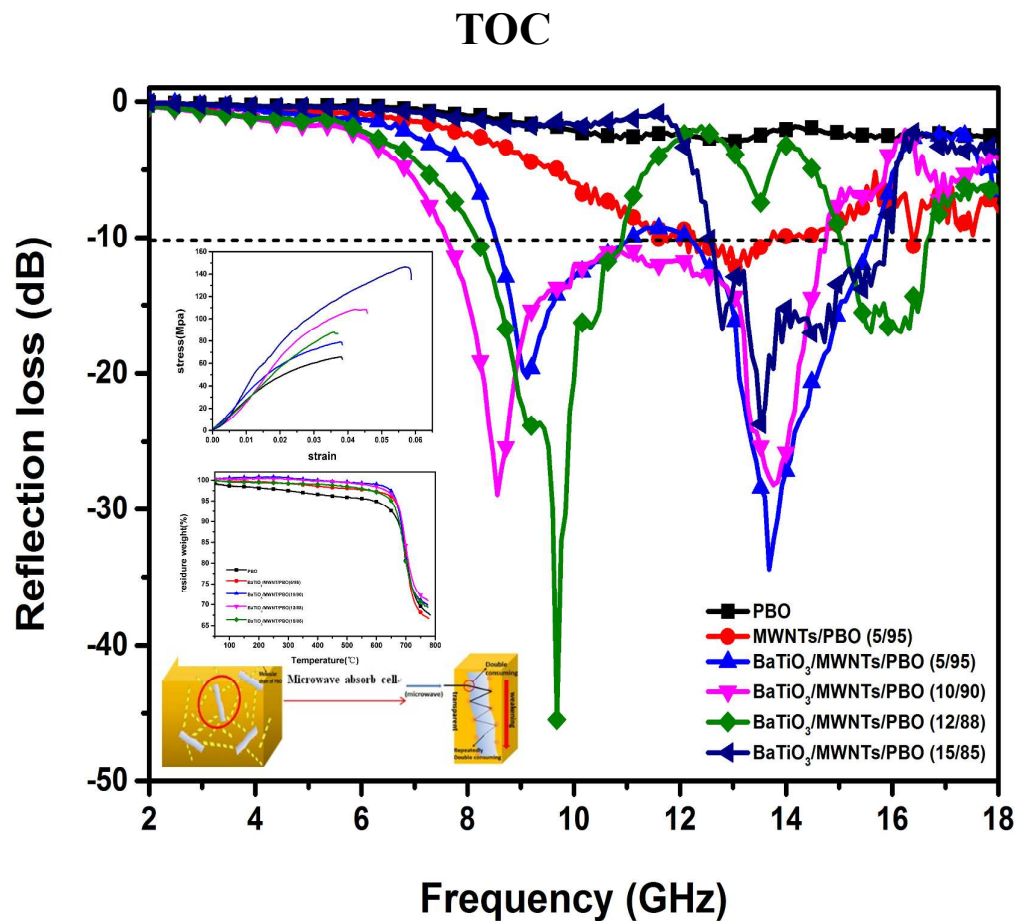
ACKNOWLEDGMENT

This work was financially supported by Basic Innovation Research Program of Science and Technology Commission of Shanghai Municipality (13JC1402002), the Innovation Program of Shanghai Municipal Education Commission (12ZZ049), Shanghai Natural Science Foundation (12ZR1407900), and China Scholarship Council.

Notes and references

- a, Key Laboratory for Specially Functional Polymers and Related Technology of Ministry of Education, School of Materials Science and Engineering, East China University of Science and Technology, Shanghai 200237, China, E-mail: qianjun@ecust.edu.cn; qxzhuang@ecust.edu.cn; Tel: +86-21-64252464
 - b, Department of Polymer Science, College of Polymer Science and Polymer Engineering, The University of Akron, Akron, Ohio 44325-3909, United States
- Electronic Supplementary Information (ESI) available: [details of any supplementary information available should be included here]. See DOI: 10.1039/b000000x
1. C. Wu, X. Huang, X. Wu, L. Xie, K. Yang and P. Jiang, *Nanoscale.*, 2013, 5, 3847.
 2. Y. H. Yu, C. C. Ma, M. K. Yu and C. Teng, *Journal of the Taiwan Institute of Chemical Engineers.*, 2014, 45, 674.
 3. D. Chen, G. S. Wang, S. He and J. Liu, *Journal of Materials Chemistry A.*, 2013, 1, 6003.
 4. T. K. Gupta, B. P. Singh, V. N. Singh, and S. Teotia, *Journal of Materials Chemistry A.*, 2014, 2, 4263.
 5. F. Qin and C. Brosseau, *Journal of Applied Physics.*, 2012, 111, 2.
 6. A. W. Orbaek, A. C. Owens, C. C. Crouse, C. L. Pint and A. R. Barron, *Nanoscale.*, 2013, 5, 9848.
 7. P. F. Zhao, C.Y. Liang, X.W. Gong, R. Gao, J.W. Liu, M. Wang, *Nanoscale.*, 2013, 5, 8022.
 8. A. Kumar, A. P. Singh, S. Kumari, P. K. Dutta, S. K. Dhawan and A. Dhar, *Journal of Materials Chemistry A.*, 2014, 2, 16632.
 9. M. M. Lu, W. Q. Cao, H.L. Shi, X. Y. Fang, J. Yang, Z. L. Hou, H. B. Jin, W. Z. Wang, J. Yuan and M. S. Cao, *Journal of Materials Chemistry A.*, 2014, 2, 10540.
 10. M. Mishra, A. P. Singh, B. P. Singh, V. N. Singh and S. K. Dhawan, *Journal of Materials Chemistry A.*, 2014, 2, 13168.
 11. K. Y. Park, J. H. Han, S. B. Lee and J. W. Yi, *Composites Part A: Applied Science and Manufacturing.*, 2011, 42, 573.
 12. J. Xiang, J. Li, X. Zhang, Q. Ye and J. Xu, *Journal of Materials Chemistry A.*, 2014, 2, 16905.

13. D. L. Zhao and X. Li, *Materials Science and Engineering B-Advanced Functional Solid-State Materials.*, 2008, 150, 105.
14. T. H. Ting, C. C. Chiang, P. C. Lin and C. H. Lin, *Applied Surface Science* 2012, 258, 3184.
15. M. N. Hyder, S. W. Lee, F. Ç. Cebeci, D. J. Schmidt, S.H. Y. and P. T. Hammond, *ACS Nano.*, 2011, 5, 8552.
16. P. Saini and M. Arora, *Journal of Materials Chemistry A.*, 2013, 1, 8934.
17. H. L. Zhu, Y. J. Bai, R. Liu, N. Lun, Y. X. Qi, F. D. Han and Bi, J.Q., *Journal of Materials Chemistry.*, 2011, 21, 135.
18. B. Wen, M. S. Cao, Z. L. Hou, W. L. Song, L. Zhang, M. M. Lu, H. B. Jin, X. Y. Fang, W. Z. Wang and J. Yuan, *Carbon.*, 2013, 65, 124.
19. C. Bi, M. Zhu, Q. Zhang, Y. Li and H. Wang, *Journal of nanoscience and nanotechnology.*, 2011, 11, 1030.
20. J. Yang, J. Zhang, C. Liang, M. Wang, P. Zhao, M. Liu and J. Liu, *ACS applied materials & interfaces.*, 2013, 5, 46.
21. Y. Chen, X. Liu, X. Mao, Q. Zhuang, Z. Xie and Z. Han, *Nanoscale.*, 2014, 6, 6440.
22. S. P. Pawar, D. A. Marathe, K. Pattabhi and S. Bose, *Journal of Materials Chemistry A.*, 2015.
23. G. Wang, Z. Gao, S. Tang, C. Chen, F. Duan, S. Zhao, S. Lin, Y. Feng, L. Zhou and Y. Qin, *ACS Nano.*, 2012, 6, 11009.
24. M. M. Lu, W. Q. Cao, H. L. Shi, X. Y. Fang, J. Yang, Z. L. Hou, H. B. Jin, W. Z. Wang, J. Yuan and M. S. Cao, *Journal of Materials Chemistry A.*, 2014, 2, 10540.
25. G. Liu, L. Wang, G. Chen, S. Hua, C. Ge, H. Zhang and R. Wu, *Journal of Alloys and Compounds.*, 2012, 514, 183.
26. Q. Su, J. Li, G. Zhong, G. Du and B. Xu, *The Journal of Physical Chemistry C.*, 2011, 115, 1838.
27. I. Nam, W. H. Lee and J. H. Jang, *Composites Part A: Applied Science and Manufacturing* 2011., 42, 1110.
28. T. K. Gupta, B. P. Singh, S. R. Dhakate, V. N. Singh, R. B. Mathur, *Journal of Materials Chemistry A.*, 2013, 1, 9149.
29. X. M. Meng, X. J. Zhang, C. Lu, Y. F. Pan, G. S. Wang, *Journal of Materials Chemistry A.*, 2014, 2, 18725.
30. Y. Z. Wei, G. S. Wang, Y. Wu, Y. H. Yue, J. T. Wu, C. Lu and L. Guo, *Journal of Materials Chemistry A.*, 2014, 2, 5516.
31. T. Fukumaru, T. Fujigaya, N. Nakashima, *Macromolecules.*, 2013, 46, 4034.
32. T. Kitagawa, H. Murase and K. Yabuki, *Journal of Polymer Science Part B: Polymer Physics.*, 1998, 36, 39.
33. Y. Chen, S. Wang, Q. Zhuang, X. Li, P. Wu and Z. Han, *Macromolecules.*, 2005, 38, 9873.
34. Z. Xie, X. Liu, Q. Zhuang, Y. Chen, X. Mao and Z. Han, *Polymer Composites.*, 2012, 33, 1295.
35. C. Bi, M. Zhu, Q. Zhang, Y. Li and H. Wang, *Materials Chemistry and Physics.*, 2011, 126, 596.
36. X. J. Zhang, G. S. Wang, Y. Z. Wei, L. Guo, M. S. Cao, *Journal of Materials Chemistry A.*, 2013, 1, 12115
37. S. He, G. S. Wang, C. Lu, J. Liu, B. Wen, H. Liu, L. Guo and M. S. Cao, *Journal of Materials Chemistry A.*, 2013, 1, 4685.
38. E. Vázquez and M. Prato, *ACS Nano.*, 2009, 3, 3819.
39. A. Q. Valenzuela and F. A. Fernandez. *Antennas and Propagation.*, 1996, 44, 822.
40. I. Najafabadi, A. Yamada, T. Futaba, D. N. Yudasaka, M. Takagi, H. Hatori, H. Iijima and S. Hata, K., *ACS Nano.*, 2011, 5, 811.
41. J. Guo, X. Wang, X. Liao, W. Zhang and B. Shi, *The Journal of Physical Chemistry C.*, 2012, 116, 8188.
42. Y. Kim, K. Kook, S. K. Hwang, C. Park and J. Cho, *ACS Nano.*, 2014, 8, 2419.
43. P. Kim, N. M. Doss, J. P. Tillotson, P. J. Hotchkiss, M. J. Pan, S. R. Marder, J. Li, J. P. Calame and J. W. Perry, *ACS Nano.*, 2009, 3, 2581.



BaTiO₃/MWNTs/PBO ternary composites with excellent microwave absorption, mechanical properties and thermostability.